International Journal of Automotive Technology, Vol. 8, No. 5, pp. 555–562 (2007)

1229–9138/2007/036–03

NONLINEAR MODEL-BASED CONTROL OF VANE TYPE CONTINUOUS VARIABLE VALVE TIMING SYSTEM

M. SON[1)], M. LEE[1)], K. LEE[2)], M. SUNWOO[3)*], S. LEE[4)], C. LEE[4)] and W. KIM[4)]

[1)]Department of Automotive Engineering, Graduate School, Hanyang University, Seoul 133-791, Korea
[2)]Automotive Control & Electronics Laboratory, Hanyang University, Seoul 133-791, Korea
[3)]Department of Automotive Engineering, Hanyang University, Seoul 133-791, Korea
[4)]Hyundai Motor Company, 772-1 Jangduk-dong, Hwaseong-si, Gyeonggi 445-706, Korea

(Received 3 January 2007; Revised 2 August 2007)

ABSTRACT–The Variable Valve Timing (VVT) system for high performance is a key technology used in newly developed engines. The system realizes higher torque, better fuel economy, and lower emissions by allowing an additional degree of freedom in valve timing during engine operation. In this study, a model-based control method is proposed to enable a fast and precise VVT control system that is robust with respect to manufacturing tolerances and aging. The VVT system is modeled by a third-order nonlinear state equation intended to account for nonlinearities of the system. Based on the model, a controller is designed for position control of the VVT system. The sliding mode theory is applied to controller design to overcome model uncertainties and unknown disturbances. The experimental results suggest that the proposed sliding mode controller is capable of improving tracking performance. In addition, the sliding mode controller is robust to battery voltage disturbance.

KEY WORDS : VVT (variable valve timing), CVVT (continuous variable valve timing), Nonlinear system, Sliding mode control

1. INTRODUCTION

The automotive industry is always trying to reduce engine fuel consumption and to improve engine performance characteristics. In addition, exhaust emission regulations have become stricter in recent years. These requirements have motivated engineers to look for solutions that allow additional degrees of freedom for the camshaft during the operation of an engine. A key step in this direction is the use of variable valve timing (VVT) systems. An engine with a VVT system can apply various cam timings over the range of engine operation. This ability improves fuel economy, reduces emissions, and increases peak torque and power (Tuttle, 1980, 1982; Leone *et al.*, 1996; Moriya *et al.*, 1996; Moro and Ponti, 2001).

To adjust cam timing according to engine conditions in real time, a VVT system requires short response time and high accuracy. In this paper, a model-based control method is proposed to enable a fast and precise VVT control system that is robust with respect to manufacturing tolerances and aging. The model is based on the physics of the system, and its parameters are identified and adjusted according to experimental data. This model is mathematically compact enough to run in real time and exhibits reasonable accuracy over a wide engine operating range.

The VVT system uses electronically controlled hydraulic actuators to change the camshaft position relative to the crankshaft position. Several previous studies have treated the VVT system as a linear system and have applied a simple linear controller (Jankovic *et al.*, 1998; Stefanopoulou *et al.*, 1998). The dynamic characteristics of the VVT system are highly nonlinear, however, and are relatively difficult to control. The nonlinearities arise from oil flow equation, oil pressure dynamics, and the dead band of the oil control valve (Merrit, 1976). Furthermore, there are many uncertainties such as cam phaser friction, load disturbance in the camshaft, and various unmodeled dynamics. The use of a sliding mode control method has been shown to be effective for controlling nonlinear systems with uncertainties (Yoon and Sunwoo, 2001), and we therefore propose its application to a VVT system.

The experimental setup is constructed to demonstrate the validity of the proposed sliding control method. The experimental results suggest that the proposed controller is capable of improving position tracking performance.

*Corresponding author. e-mail: msunwoo@hanyang.ac.kr

2. OVERVIEW OF THE VVT SYSTEM

The CVVT system consists of two main components: an oil control valve (OCV) and a cam phaser. A continuous variable valve timing (CVVT) unit is used in this paper as a cam phaser (Kim *et al.*, 2006). The CVVT unit shown in Figure 1 is a hydraulic vane-type actuator. The stator is driven by the crankshaft, and the rotor with radially projecting vanes is mechanically coupled to the camshaft. The camshaft is moved relative to the stator by one-side loading of the vanes due to oil pressure.

Figure 2 is a schematic of the CVVT system. The CVVT unit has two oil chambers: an advance chamber and a retard chamber. The chambers are named according to the direction of the cam timing when the chamber is filled. Accordingly, filling the advance chamber causes the rotor of CVVT unit and cam shaft to move toward the advanced timing position, and vice versa for the retard chamber. The OCV consists of a spool valve and an electromagnetic solenoid. The spool valve controls the rate and direction of the oil flow applied to the oil chamber. The spool position is determined by the electromagnetic solenoid, which is driven by the pulse width modulation (PWM) signal.

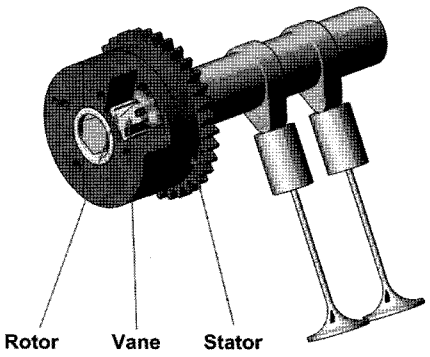

Figure 1. CVVT unit.

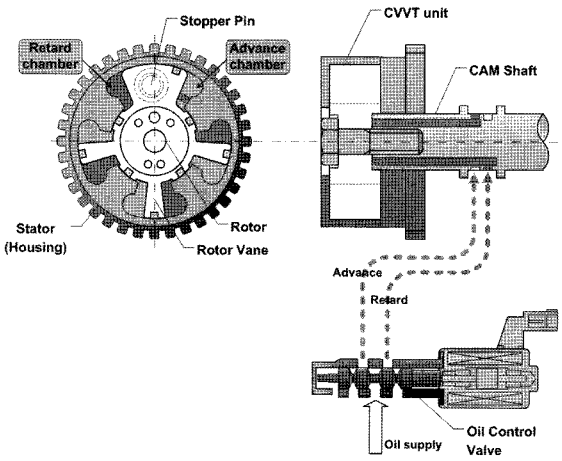

Figure 2. Configuration of CVVT system.

3. MATHEMATICAL MODEL OF CVVT SYSTEM

A model of the CVVT system for model-based control has been developed. This model is mathematically compact enough to be easily applied to the controller design and to run in real time, and exhibits reasonable accuracy against actual cam phasing characteristic. For simplicity, the model operates on the following assumptions:

- Oil leakage does not occur.
- The return pressure is equal to the atmospheric pressure.
- The cavitation effect is ignored.
- The OCV orifices are symmetrical.
- The OCV valve is regarded as a zero-order system.

The mathematical model of CVVT system is developed based on physical laws. Figure 3 is a diagram of the system model. The oil's flow direction and flow rate are determined by the spool displacement x_v of the OCV. This oil flow changes the pressure of both chambers, P_1 and P_2. The difference between the chamber pressures P_1 and P_2 drives the vane movement, and vane displacement thus in turn determines cam timing.

The mathematical model is made up of the spool valve flow sub-model, the chamber pressure sub-model, and the cam phaser sub-model.

3.1. Spool Valve Flow Sub-model

Flow rates Q_1 and Q_2 through the spool valve orifices are described by the orifice law, which incorporates Bernoulli's equation, the continuity equation for incompressible flow, and an empirical factor (Merrit, 1976; Zhang *et al.*, 2007):

$$Q_1 = \begin{cases} C_d w x_v \sqrt{\frac{2}{\rho}(P_s - P_1)}, & x_v \geq 0 \\ C_d w x_v \sqrt{\frac{2}{\rho}(P_1 - P_r)}, & x_v < 0 \end{cases} \quad (1)$$

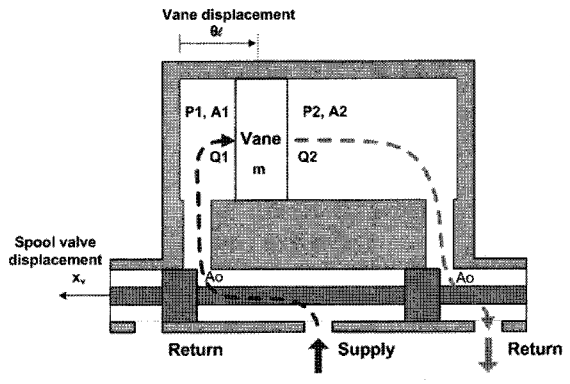

Figure 3. Modeling diagram of CVVT system.

$$Q_2 = \begin{cases} -C_d w x_v \sqrt{\frac{2}{\rho}(P_2 - P_r)}, & x_v \geq 0 \\ -C_d w x_v \sqrt{\frac{2}{\rho}(P_s - P_2)}, & x_v < 0 \end{cases} \quad (2)$$

where C_d is the discharge coefficient, w is the spool's port width, x_v is the spool displacement, ρ is the engine oil density, P_1 and P_2 are chamber pressures, P_s is the supply pressure from the oil pump, and P_r is the return pressure.

The load flow Q_L is defined by $Q_L=(Q_1+Q_2)/2$, and the load pressure $P_L=P_1-P_2$ is the pressure drop across the load. Therefore, the spool valve flow sub-model can be expressed as follows:

$$Q_L = C_d w x_v \sqrt{\frac{P_s - \mathrm{sgn}(x_v) P_L}{\rho}} \quad (3)$$

In this study, OCV dynamics is simplified so that the control input u is proportional to the spool displacement; that is, $x_v=k_v u$, where k_v is the valve gain. This assumption is reasonable because the OCV response is much faster than the rest of the VVT system components. The parameter k_v is identified by experiment.

3.2. Chamber Pressure Sub-model

The chamber pressure dynamics can be described by applying the continuity equation to both chambers

$$\dot{P}_1 = \frac{\beta_e}{V_1}\left(-\dot{V}_1 + Q_1\right) \quad (4)$$

$$\dot{P}_2 = \frac{\beta_e}{V_2}\left(-\dot{V}_2 + Q_2\right) \quad (5)$$

where β_e is the effective bulk modulus of the engine oil. The two chamber volumes are given by

$$V_1 = V_{10} + l\theta A_1 \quad (6)$$

$$V_2 = V_{20} + l(\theta_t - \theta) A_2 \quad (7)$$

where V_{10} and V_{20} are the initial volumes of each chamber, including valve volume, connecting line volume, and chamber volume, l is the length between the rotor center and the center of gravity of the vane, θ is the angular vane position, θ_t is the total angular displacement of the vane, and A_1 and A_2 are the vane areas.

By adding equations (6) and (7), the total contained volume of both chambers is given by $V_t=A_1+A_2$. Therefore, the chamber pressure sub-model can be expressed as follows:

$$\dot{P}_L = \frac{4\beta_e}{V_t}\left(Q_L - Al\dot{\theta}\right) \quad (8)$$

3.3. Cam Phaser Sub-model

The cam phaser dynamics can be described by applying Newton's Second Law to the forces applied to the rotor. The resulting force equation is given by

$$AP_L = M_t l\ddot{\theta} + bl\dot{\theta} + kl\theta + F_f \quad (9)$$

where M_t is the total mass of rotor and load referred to the rotor, is the viscous damping coefficient of the rotor and load, is the spring constant, and is the friction force.

3.4. State Space Models

Combining the three sub-models, the mathematical model of the CVVT system is modeled by the following state equation:

$$\begin{aligned} \dot{x}_1 &= x_2 \\ \dot{x}_2 &= x_3 \\ \dot{x}_3 &= f(\mathbf{x},t) + g(\mathbf{x},t)u(t) + d(t) \\ &= \sum_{i=1}^{3} a_i(t) x_i(t) + g(\mathbf{x},t)u(t) + d(t) \end{aligned} \quad (10)$$

where

$$\mathbf{x} = \begin{bmatrix} x_1 & x_2 & x_3 \end{bmatrix}^T = \begin{bmatrix} \theta & \dot{\theta} & \ddot{\theta} \end{bmatrix},$$

$$a_1 = 0, \quad a_2 = -\frac{k}{M_t} - \frac{4\beta_e A^2}{M_t V_t}, \quad a_3 = -\frac{b}{M_t},$$

$$g(\mathbf{x},t) = \frac{4\beta_e A}{M_t V_t l} C_d w k_v \sqrt{\frac{P_s - \mathrm{sgn}(x_v) P_L}{\rho}},$$

$$d(t) = -\frac{1}{M_t l} F_f$$

The vector $\mathbf{x}$ is the state vector of the system, and the scalar u is the control input. The state variables are the vane angular position, angular velocity, and angular acceleration. The friction force F_f is considered to be the external disturbance. The input signal to the VVT system is the PWM signal used for driving the OCV. The measurable output signal is the vane angular position, which can be acquired by measurement of the cam phase and crank phase.

4. EXPERIMENTAL SETUP

The experimental setup is constructed to identify model parameters and validate the proposed controller. Figure 4 is a schematic of the experimental setup, which consists of the engine equipped with a VVT system, the data acquisition system, and the VVT electronic control unit (ECU). Figure 5 shows a photograph of the engine. The test engine is fitted with a direct-current dynamometer. An absolute optical encoder with 12-bit binary output and an incremental optical encoder are mounted to the intake camshaft and crankshaft, respectively. When the engine is running, these encoders are used to measure cam timing accurately and in real time.

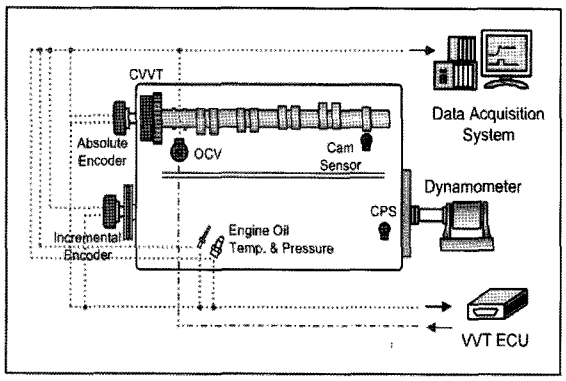

Figure 4. The schematic of the experimental setup.

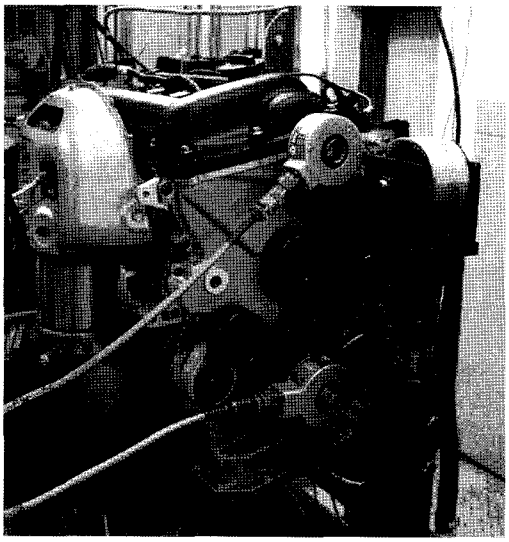

Figure 5. Photograph of engine equipped with a VVT system.

The ECU for the VVT system is implemented using the dSPACE's MicroAutoBox, a rapid control prototyping (RCP) system. By using this system, the development and implementation of the controller can easily be accomplished in MATLAB®/Simulink®. This ECU controls the VVT system by feedback of cam and crank phase signal data, which are generated by the shaft encoders.

The data acquisition system consists of a data acquisition board and a LabVIEW program (National Instruments). The data acquisition process is triggered at every 1 °CA by a signal from the crank shaft encoder. The sensor signals, such as engine oil temperature, engine oil pressure and the cam phase signal from camshaft encoder, are acquired and stored.

5. SLIDING MODE CONTROLLER DESIGN

In this paper, the sliding mode control method is proposed as a means of designing a controller suited for the nonlinear dynamics of the VVT system. This method is directly applicable to a set of nonlinear dynamic equations and directly considers the robustness to model uncertainties and disturbances in the design process. These features make this method highly desirable for designing a closed-loop VVT system controller.

5.1. Problem Formulation

Recall the controllable canonical form of the nonlinear VVT system model from equation (10) as

$$\begin{aligned}\dot{x}_1&=x_2\\ \dot{x}_2&=x_3\\ \dot{x}_3&=f(\mathbf{x},t)+g(\mathbf{x},t)u(t)+d(t)\end{aligned} \tag{10}$$

where $\mathbf{x}=[x_1\ x_2\ x_3]^T \in \mathbf{R}^{3\times 1}$ is a state vector, $u(t) \in \mathbf{R}^1$ is a scalar control input, $d(t) \in \mathbf{R}^1$ is a scalar disturbance, and $f(\mathbf{x}, t)$ and $g(\mathbf{x}, t)$ are the system parameters and the control gain respectively, representing nonlinear functional relationships. To quantify robustness with respect to model uncertainties and disturbances, define:

$$\begin{aligned}f(\mathbf{x},t)&=\hat{f}(\mathbf{x},t)+\Delta f(\mathbf{x},t)\\ g(\mathbf{x},t)&=\hat{g}(\mathbf{x},t)+\Delta g(\mathbf{x},t)\\ d(t)&<D\end{aligned} \tag{11}$$

where $\hat{f}(\mathbf{x},t)$ and $\hat{g}(\mathbf{x},t)$ are the nominal system parameters, $\Delta f(\mathbf{x},t)$ and $\Delta g(\mathbf{x},t)$ are parameter uncertainties, and D is the disturbance upper bound.

The system parameter uncertainty can be bounded by a known function F:

$$|\Delta f(\mathbf{x},t)|<F(\mathbf{x},t). \tag{12}$$

The control gain $g(\mathbf{x},t)$ is not completely known, but is bounded as follows:

$$0<g_{\min}\le g(\mathbf{x},t)\le g_{\max} \tag{13}$$

where $g_{\min}$ and $g_{\max}$ are given constants. Since the control input is multiplied by the control gain in the dynamics, the control gain g is estimated to be the geometric mean of the lower and upper bounds of the gain:

$$\hat{g}=\frac{1}{\sqrt{g_{\min}\cdot g_{\max}}} \tag{14}$$

The control problem is defined as tracking $x_1(t)$ to a desired trajectory, $x_{1d}(t)$, in the presence of model uncertainties and disturbances. The tracking error is given by:

$$e(t)=x_1(t)-x_{1d}(t) \tag{15}$$

The desired error dynamics can be defined by a sliding surface $s(t)=0$ where $s(t)$ is as follows:

$$s(t)=\left(\frac{d}{dt}+\lambda\right)^2 e=\lambda^2 e+2\lambda\dot{e}+\ddot{e} \tag{16}$$

and λ is a strictly positive constant chosen so that $s(t)=0$ yields acceptable error dynamics.

5.2. Controller Design

The control law must satisfy a sliding condition (Utkin *et al.*, 1999; Chun and Sunwoo, 2004):

$$s(t)\dot{s}(t) \le -\eta|s(t)| \tag{17}$$

If the control input, $u(t)$, can be chosen to satisfy the sliding condition for a strictly positive η, then the system will reach the sliding surface ($s(t)=0$) within a finite time t_r computed by

$$\dot{s}(t)=-\eta\text{sgn}(s(t))$$
$$\int_0^{t_r} -\eta\text{sgn}(s(t))d\tau=-s(0) \Rightarrow t_r=\frac{|s(0)|}{\eta} \tag{18}$$

and slide along $s(t)=0$.

Differentiation of $s(t)$ with respect to t yields:

$$\dot{s}(t)=\lambda^2\dot{e}+2\lambda\ddot{e}+f(\mathbf{x},t)+g(\mathbf{x},t)u(t)+d(t) \tag{19}$$
$$=-\eta\text{sgn}(s(t))$$

The control law that satisfies the sliding condition can be solved from equation (19) as follows:

$$u(t)=-\hat{g}^{-1}(\mathbf{x},t)[\hat{u}+K\text{sgn}(s)] \tag{20}$$

where

$$\hat{u}(t)=\lambda^2\dot{e}+2\lambda\ddot{e}+\hat{f}(\mathbf{x},t)-\ddot{x}_{1d},$$

the sliding gain K is defined as:

$$K \equiv \beta(F+\eta)+(\beta-1)|U|+D$$
$$|f-\hat{f}|<F(\mathbf{x},t);|\hat{u}|<U;|d|<D,$$

and the gain margin β as:

$$\beta=\sqrt{g_{\max}/g_{\min}},$$
$$g^{-1} \le \frac{\hat{g}}{g} \le \beta$$

Assuming that the coefficients of the state equation (10) may fluctuate up to 50% from their nominal values, the bounds of the uncertainties and the estimation error can be determined:

$$\beta=\sqrt{g_{\max}/g_{\min}}=\sqrt{(\hat{g}\cdot 1.5)/(\hat{g}\cdot 0.5)}=\sqrt{3}$$
$$F=|f-\hat{f}|=0.5|\hat{f}|$$

The sliding mode switching control law guarantees that the sliding condition is satisfied even in the presence of model uncertainties and unknown disturbances.

Discontinuous switching control usually results in chattering, which may excite undesirable high frequencies or unmodeled dynamics. Chattering can be alleviated by a smoothing approximation in the boundary layer neighboring the sliding surface, $s(t)=0$. A simple method is to replace a sign function with the following saturation function (Utkin *et al.*, 1999):

$$\text{sgn}(s(t)) \rightarrow \text{sat}\left(\frac{s(t)}{\phi}\right) \text{ with } \phi>0 \tag{21}$$

where ϕ is the thickness of the boundary layer, which should be adjusted to achieve an optimal balance of tracking performance and chatter reduction. The resulting control law is written as follows:

$$u(t)=\hat{g}^{-1}(\mathbf{x},t)[\hat{u}+K\text{sgn}(s/\phi)] \tag{22}$$

In this control law, chatter is alleviated even though $s(t)$ may not tend towards zero. The resulting control law therefore guarantees that the system will reach the boundary layer within a finite time t_r and remain ultimately bounded in the neighborhood of the origin.

6. EXPERIMENTAL RESULTS

Two different approaches to control are presented for performance comparison. First, a linear PID controller expressed as follows:

$$u=K_P+\frac{K_I}{s}+K_D s \tag{23}$$

where K_P, K_I and K_D are given fixed gains. A second controller is designed using a sliding mode control method. The control law is a modification of equation (22):

$$u(t)=\hat{g}^{-1}(\mathbf{x},t)[\hat{u}+K\tanh(s/\phi)] \tag{24}$$

To evaluate the position control performance of the VVT system, various test conditions were carried out: step inputs, sinusoidal input, and battery voltage disturbances. The experiment was performed at 1500, 2000 and 2500 RPM. The experimental results only for 2000 RPM are presented because the experimental results for 1500-2500 RPM are almost the same.

First, the desired tracking inputs are set to be step inputs. Both a small and a large step size are applied at the references of the both controllers. For the small step input, the intake cam phaser was moved from 5°CA to 20°CA, and then back to 5°CA. On the other hand, for the large step input, the cam phaser was moved from 5°CA to 45°CA, and then back to 5°CA. Figures 6(a) and (b) show the tracking outputs for the desired cam timing conditions. In Figures 6(a) and (b), the linear PID controller is seen to suffer from a slow settling time and large tracking error. Moreover, tracking error increased with the large step input (Figure 6(b)). By contrast, the proposed sliding mode controller exhibited a much faster settling time and small tracking error.

The next test used a sinusoidal input with a period of 4 seconds, and an amplitude of 35°CA from 5°CA to 40°CA. Figure 7 shows the tracking outputs for the

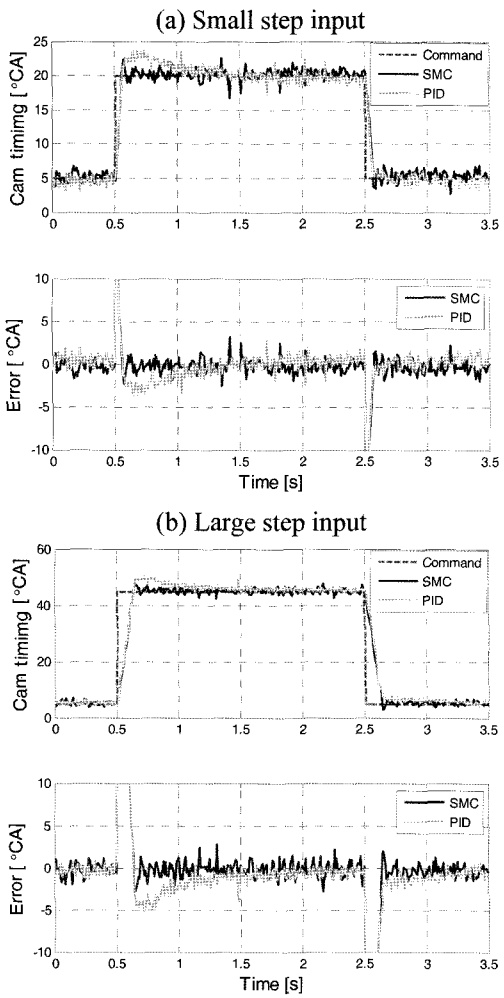

Figure 6. Tracking performance for step inputs.

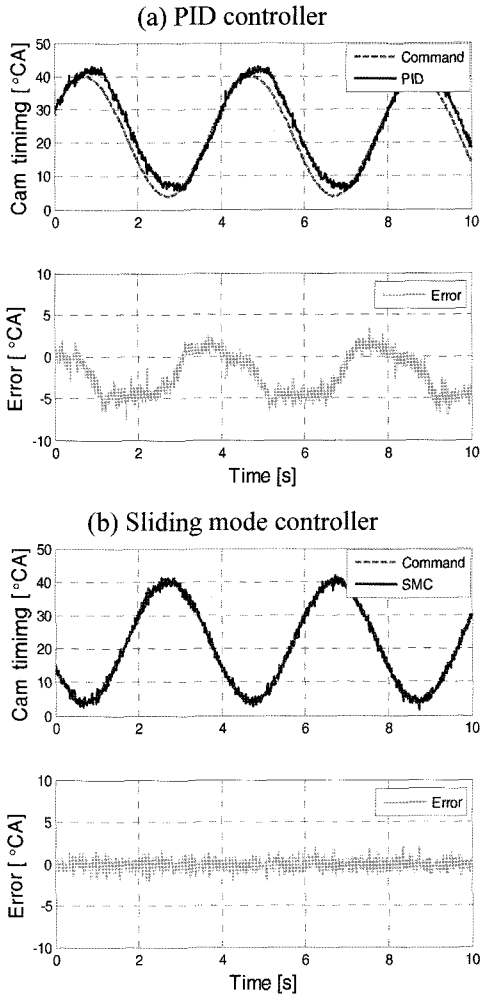

Figure 7. Tracking performance for sinusoidal input.

sinusoidal input. In this test, the sliding mode controller exhibited remarkably better tracking performance than the PID controller.

The OCV control current is influenced by battery voltage and controlled by the PWM signal from ECU command. In the modeling process, the OCV dynamics are assumed to be a zero-order system and the influence of battery voltage is ignored. The battery voltage can be changed by vehicle operating conditions. In this test, a battery voltage disturbance is applied to both controllers.

Figures 8(a) and (b) show the influence of a rising step disturbance with a cam timing command of 20°CA. For the linear PID controller, cam timing was changed at the rising edge of battery voltage and then tracked to command with a settling time of 3 seconds. However, the proposed sliding mode controller was not affected by the step change in battery voltage.

Figure 9 shows the influence of the voltage swing that was applied from 10 V to 13.5 V with a cam timing command of 40°CA. In this test, the proposed sliding mode controller exhibited a smaller tracking error than the PID controller.

In general, the tracking performance of the sliding mode controller was better than that of the PID controller and also was more robust to changes in battery voltage.

7. CONCLUSIONS

The dynamic characteristics of the VVT system are highly nonlinear and are relatively difficult to control. Furthermore, there are many model uncertainties and unknown disturbances. Therefore, the model should account for nonlinear dynamics, and the proposed controller should be able to control the nonlinear CVVT system despite model uncertainties and unknown disturbances. An experiment was carried out to evaluate the performance of the control method.

The major conclusions are summarized as follows:

(1) The CVVT system model was developed for real-

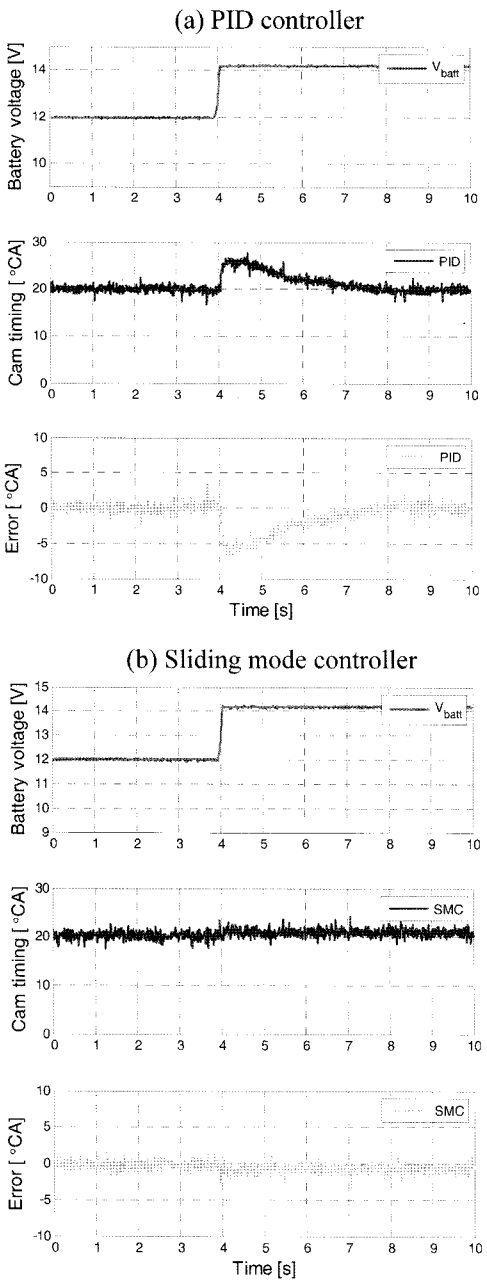

Figure 8. Battery voltage step input.

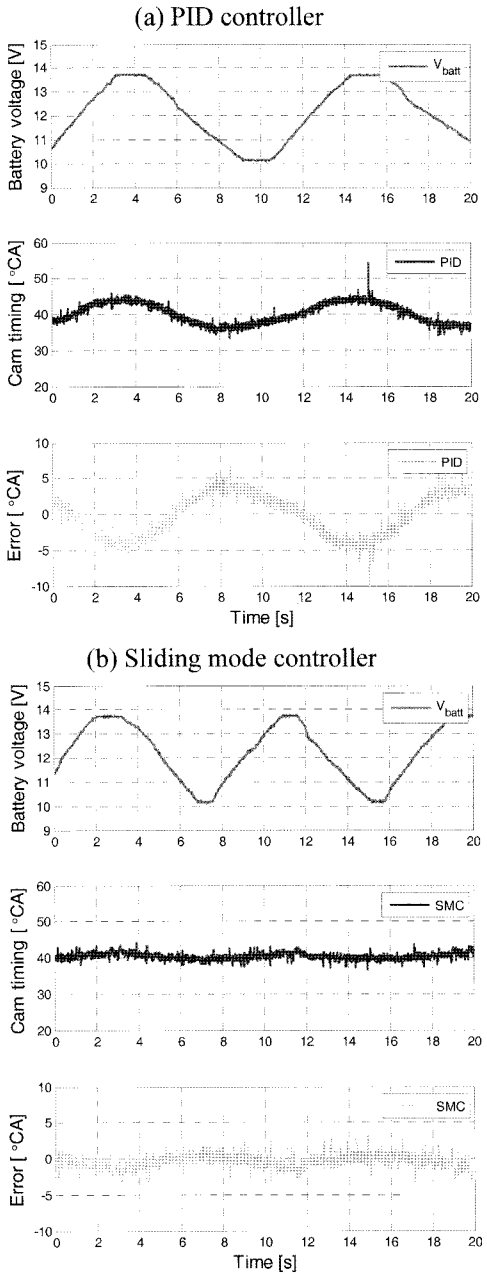

Figure 9. Battery voltage swing.

time control. This simplified model is represented as a third-order nonlinear state equation. The parameters were adjusted by using experimental data.

(2) The sliding mode controller was designed for the nonlinear dynamics of the VVT system. This controller was proposed because of its robustness in handling model uncertainties and unknown disturbances.

(3) Experimental results showed that the proposed sliding mode controller is capable of improving the tracking performance. The proposed sliding mode controller was much better than the linear PID controller for tracking performance and also for providing fast response and high precision for the position control of the nonlinear VVT system. In addition, the sliding mode controller was robust to battery voltage disturbances.

ACKNOWLEDGMENTS–This research is supported by the MOST (Ministry of Science and Technology) under the

National Research Laboratory (NRL) program and by the MOCIE (Ministry of Commerce, Industry and Energy) under the "Development of Engine System for Hybrid Vehicle" project. We are grateful for their financial support.

REFERENCES

Chun, K. and Sunwoo, M. (2004). Wheel slip control with moving sliding surface for traction control system. *Int. J. Automotive Technology* **5**, **2**, 123–133.

Jankovic, M., Frischmuth, F., Stefanopoulou, A. G. and Cook, J. A. (1998). Torque management of engines with variable cam timing. *IEEE Control Systems Magazine,* **18**, 34–42.

Kim, J., Kim, H. and Jeon, C. (2006). Developement of high performance gasoline engine for small & middle car. *Spring Conf. Proceedings*, **I**, *Korean Society of Automotive Engineers*, 112–117.

Leone, T. G., Christenson, E. J. and Stein, R. A. (1996). Comparison of variable camshaft timing strategies at part load. *SAE Paper No.* 960584.

Merrit, H. E. (1976). *Hydraulic Control Systems*. Wiley. U.S.A.

Moriya, Y., Watanabe, A., Uda, H., Kawamura, H. and Yoshioka, M. (1996). A newly developed intelligent variable valve timing system - Continuously controlled cam phasing as applied to an new 3 liter inline 6 engine. *SAE Paper No.* 960579.

Moro, D. and Ponti, F. (2001). Thermodynamic analysis of variable valve timing influence on SI engine efficiency. *SAE Paper No.* 2001-01-0667.

Stefanopoulou, A. G., Cook, J. A., Grizzle, J. W. and Freudenberg, J. S. (1998). Control-oriented model of a dual equal variable cam timing spark ignition engine. *J. Dynamic Systems, Measurement and Control*, **120**, 257–266.

Tuttle, J. H. (1980). Controlling engine load by means of late intake-valve closing. *SAE Paper No.* 800794.

Tuttle, J. H. (1982). Controlling engine load by means of early intake-valve closing. *SAE Paper No.* 820408.

Utkin, V., Guldner, J. and Shi, J. (1999). *Sliding Mode Control in Electromechanical Systems*. Taylor & Francis. U. K.

Yoon, P. and Sunwoo, M. (2001). An adaptive sliding mode controller for air-to-fuel ratio control of spark ignition engines. *Proc. Institution of Mechanical Engineers-Part D* **215**, **D5**, 305–315.

Zhang, Y. X., Zhang, J. W., Shangguan, W. B., and Feng, Q. SH. (2007). Modeling and parameter identification for a passive hydraulic mount. *Int. J. Automotive Technology* **8**, **2**, 233–241.